Scientific Research Publishing

International Journal of Geosciences, 2026, 17(11), 851-882
https://www.scirp.org/journal/ijg
ISSN Online: 2156-8367
ISSN Print: 2156-8359

Was the Ravne Underground Complex Once a Single Network? Entrance Levels, Passage Orientation, and Valley Incision in Six Tunnel Systems, Visoko, Bosnia and Herzegovina

Sam Osmanagich

Archaeological Park: Bosnian Pyramid of the Sun Foundation, Visoko, Bosnia and Herzegovina
Email: info@drsamosmanagich.com

How to cite this paper: Osmanagich, S. (2026) Was the Ravne Underground Complex Once a Single Network? Entrance Levels, Passage Orientation, and Valley Incision in Six Tunnel Systems, Visoko, Bosnia and Herzegovina. *International Journal of Geosciences*, **17**, 851-882.
https://doi.org/10.4236/ijg.2026.1711040

Received: October 12, 2026
Accepted: November 17, 2026
Published: November 20, 2026

Copyright © 2026 by author(s) and Scientific Research Publishing Inc.
This work is licensed under the Creative Commons Attribution International License (CC BY 4.0).
http://creativecommons.org/licenses/by/4.0/

Open Access

Abstract

Six tunnel systems, Ravne 1 to Ravne 6, lie within 0.6 km of each other near Visoko. We test whether they are surviving parts of one former network. We used the 5191 floor points of the 2026 GeoGIS survey. The systems hold 2453 m of mapped passage. All six entrances lie between 470.04 and 471.50 m a.s.l., a spread of 1.46 m. Each entrance floor lies within 0.11 m of its system's lowest recorded floor, and inner floors rise 0.4 - 4.0 m above the entrances. Any two entrances could be joined by a straight line at 1.02% or less. Of 45 terminal passage ends, 20 point within 35˚ at a neighboring system. A Monte Carlo test shows that random orientations give the same number (19.0 ± 3.1; $p = 0.44$), so passage orientation does not support a former network. Two null models that keep each system's own directional pattern give the same result. One pair of ends, in Ravne 1 and Ravne 5, faces each other about 50 m apart at nearly matching floor level. A second mutual pair, between Ravne 4 and Ravne 6, differs by 2.1 m in level. Two or more mutual pairs occurred in 17% of null simulations. The valley of Park Ravne 2 lies 4 - 19 m below tunnel level. The narrow range of present entrance and floor elevations is consistent with coordinated vertical planning, although the surveyed floors are cleared surfaces whose original integrity is not established. It cannot by itself distinguish a formerly connected network from separate excavations at a common geological or topographic level. We define the tests that can.

Keywords

Ravne Tunnels, Underground Network, Entrance Level, Passage Orientation, Monte Carlo Test, Valley Incision, Terrestrial Laser Scanning, Visoko

1. Introduction

The Ravne locality near Visoko holds six mapped tunnel systems, Ravne 1 to Ravne 6 (Figure 1, Figure 2). Each has its own entrance. No open passage joins any two of them today. In earlier papers Ravne 1 appears as "Ravne".

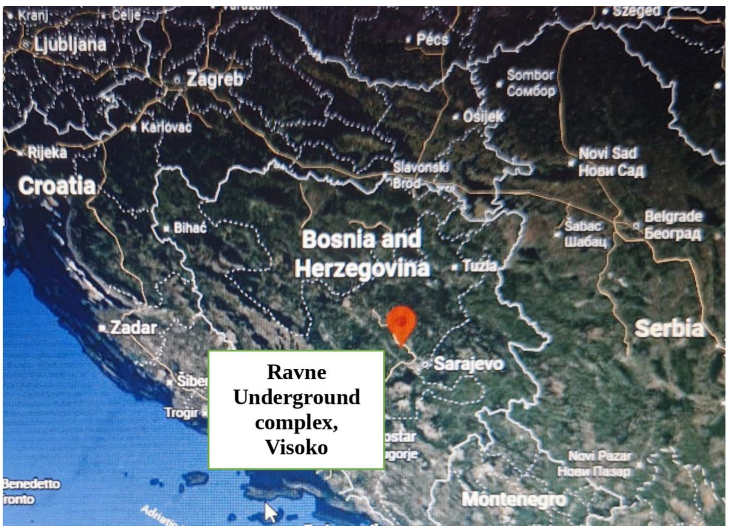


Figure 1. Location of the Ravne Underground Complex, Visoko, central Bosnia and Herzegovina. Adapted from [2], CC BY 4.0.

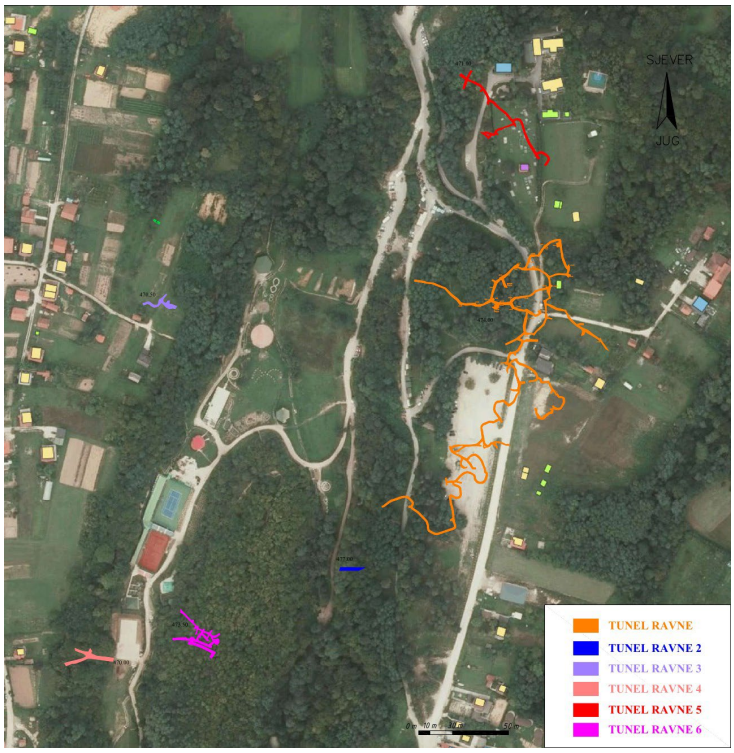


Figure 2. Composite plan of tunnels Ravne 1 ("Tunel Ravne") to Ravne 6 on satellite imagery, with Park Ravne 2 in the central valley. Foundation geodetic composite, 2025. Passage extents shown predate the 2026 survey; the geometry analyzed here is that of the 2026 survey.

The systems share construction traits. Passages have similar cross-sections and junction forms where they have not been enlarged for timber support (Section 3.6). Side passages are closed with dry-stone walls, and long sections are packed with anthropogenic backfill [1]-[4]. More than 60 river-pebble dry-stone walls are recorded in Ravne 1, 3, 4, and 6 [1]. Clearing since 2007 has followed backfill in Ravne 1, 3, 4, 5, and 6. Only Ravne 2 ends against intact rock.

Earlier work noted that the Ravne 1 and Ravne 3 entrances lie at nearly the same elevation, about 200 m apart across the valley [1]. A 2023 ground-penetrating radar survey found anomalies read as blocked or unexcavated tunnel segments [1]. The 2026 GeoGIS survey placed all six systems in one geodetic frame and recorded floor levels throughout [5] [6]. Their spatial relations can now be tested.

We ask one question. Are Ravne 1 - 6 six independent works, or surviving parts of one network later cut apart? Three hypotheses are tested (**Table 1**). They are not exclusive. Some systems could have been joined and others not.

Table 1. Hypotheses and their predictions.

Hypothesis	Claim	Predicts
H1 Former single network	The systems were once joined; links were later backfilled or destroyed by valley incision	One datum for all portals and floors; passage ends facing neighbors more often than chance; missing ground where links would run
H2 Common geological horizon	Separate tunnels followed one favorable layer	Floor levels track the conglomerate-marl unconformity, including where it rises or falls
H3 Separate adits from an existing valley	Each system was driven into the valley side from a common working level	Portals at one level on the valley flanks; passage ends with no preferred direction toward neighbors

2. Study Area, Geology and Chronology

The tunnels lie in cadastral municipality Kraljevac, Visoko, about 30 km north-west of Sarajevo. A north-south valley, now Park Ravne 2, separates two wooded slopes. Ravne 1 and Ravne 5 lie in the eastern slope. Ravne 3 lies in the western slope, opposite Ravne 1. Ravne 6 lies about 280 m south of Ravne 3, and Ravne 4 just west of Ravne 6. The short Ravne 2 lies at the southern end of the valley.

The Visoko Valley lies in the Inner Dinarides [7], within the Miocene intramontane basin system of the Central Dinarides [8]. The tunnels are cut into a horizontally bedded Quaternary unit, informally the Ravne Conglomerate Formation, of rounded quartzite, limestone, and metamorphic cobbles in a clay-rich matrix. It rests with angular unconformity on north-west-dipping Miocene marl and sandstone ([1]; **Figure 3**). Several passages run with a conglomerate ceiling and a marl floor [1] [9]. A 2015 airborne LiDAR model showed even slopes and no topographic barrier between Ravne 1 and Ravne 3 [1].

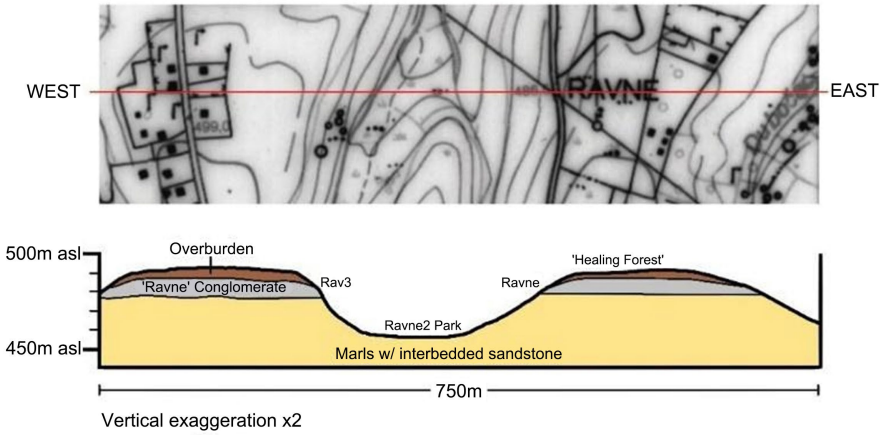


Figure 3. West-east geological section across the Ravne valley: Ravne Conglomerate over Miocene marls with interbedded sandstone, with Ravne 3 ("Rav3") and Ravne 1 ("Ravne") on opposite flanks of Park Ravne 2. Vertical exaggeration ×2. Drawing by R. Hoyle, from [1].

The dated speleothems come from inside the tunnel system. They are conical stalagmites standing on passage floors in blocked side passages of Ravne 3, next to dry-stone walls [1] [9] [10]. They are not from a separate karst cavern. The host conglomerate contains limestone cobbles, a plausible source of the carbonate in percolating water. Uranium-thorium ages are 19,000 ± 1000 years BP (US001), 15,000 ± 1000 years BP (S008) and 5900 ± 300 years BP (S002, basal age) [9] [10]. Radiocarbon dates on charcoal from backfill and wall contexts fall in the 3rd - 4th centuries CE [1] [2]. A U-Th age dates the start of carbonate growth and so gives a minimum age for the open space in which a speleothem grew [11] [12].

3. Data and Methods

3.1. Survey

GeoGIS studio d.o.o. Sarajevo surveyed the complex in 2026 [5]. Fifteen control points (GG1 - GG15) and four traverse points (T1 - T4) were fixed by GNSS (Tersus Oscar and Luka, network RTK, 10 epochs, three separate observation cycles averaged; stated accuracy 8 mm + 0.5 ppm horizontal, 15 mm + 0.5 ppm vertical; achieved vertical RMS 0.02 - 0.03 m). The surface was flown with a DJI Zenmuse L2 LiDAR on a Matrice 350 RTK. The tunnels were scanned with Trimble X7 and TX8 scanners from about 719 stations, registered in Trimble RealWorks, and tied to the control network through the UAV LiDAR cloud (**Figure 4**). Terrestrial laser scanning is an established method for documenting tunnel geometry [13], and airborne LiDAR for mapping archaeological landscapes beneath vegetation [14] [15]. Low sections of Ravne 4 and of meditation route 2, and flooded parts of Ravne 1, where water-bearing sections are documented [16], could not be scanned. Coordinates are in MGI/Balkans zone 6 (EPSG:31276); Y is easting and X is northing. All elevations are in m a.s.l.; the sketches label them "mnv".

Control was measured by network RTK through FBiHPOS, the permanent

GNSS station network of the Federal Administration for Geodetic and Real Property Affairs. Horizontal coordinates are in the state system on the Bessel 1841 ellipsoid, reached by a seven-parameter transformation adopted from the Visoko municipal survey office. Heights are in BH_VRS1971.5 [17], the inherited vertical reference system of the Federation of Bosnia and Herzegovina. It derives from the second high-accuracy levelling and refers to mean sea level at five Adriatic tide gauges, epoch 1971.5 [18]. The tunnels were tied to this frame in two steps. The UAV LiDAR cloud was fitted to the control points, and the TLS cloud of each tunnel was then fitted separately to the LiDAR cloud over the ground around its entrance [17]. All six systems therefore share one frame, and any datum offset cancels in inter-system differences.

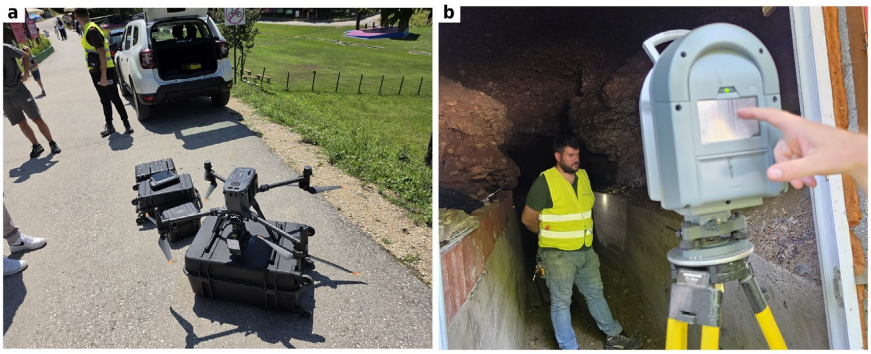


Figure 4. 2026 field survey. (a) DJI Matrice 350 RTK with Zenmuse L2 LiDAR before the flight over Park Ravne 2. (b) Trimble X7 scanning at the Ravne 2 entrance.

Floor heights are taken directly from the GeoGIS point lists (Section 3.3). Their uncertainty differs between comparisons within one system and comparisons between systems. Within a system, all points share one registration. The error there comes from floor roughness and from any error accumulated along the scan chain. Floor points within 1 m of each other have a median standard deviation of 0.04 m (90th percentile 0.14 m). GeoGIS closed scan loops at junctions to limit accumulation but reports no closure residuals. Between systems, each tunnel carries its own tie error. The control points have a GNSS vertical RMS of 0.02 - 0.03 m. The LiDAR cloud matches 12 control points with a vertical RMSE of 0.062 m and four further points with 0.047 m. The TLS clouds match the LiDAR with cloud-to-cloud errors of 0.031 - 0.035 m per tunnel [17]. RealWorks reports small overlaps (0% - 7%) and low confidence for three of the six fits, because the LiDAR cloud covers a far larger area than the entrance zones. Treating the LiDAR and cloud-to-cloud errors as independent at each tie, which is conservative, gives about ±0.07 m (1σ) for the level of one system and about ±0.10 m for a difference between two. Differences above about 0.3 m (3σ) are resolved. Three of the 15 entrance-to-entrance differences (0.04 - 0.17 m; Section 4.3) are not, and are treated as equal within error. The 1.46 m entrance spread is well above this level; the 0.4 m floor difference of link L1 (Section 4.4) is only just above it.

3.2. Data Used

- Tunnel-axis lists for Ravne 1 - 6 (98, 2, 24, 10, 15, and 26 points; Y and X).
- Control and traverse points (19 points; Y, X, and H).
- Geodetic sketches of each system at 1:2500, drawn from the point clouds (**Figures 5-7**). Each gives a summary box (length, plan area, volume, lowest and highest floor, and mean floor gradient), the entrance (ULAZ), and floor spot heights along every passage.
- Point lists exported by GeoGIS from the point clouds: 5191 floor points and 20217 ceiling points (none for Ravne 2), with coordinates and heights to 1 mm.



Figure 5. Geodetic sketch of Ravne 1, sheet 1: 1706.5 m of passage, mean gradient 1.0%, entrance floor 471.50 m a.s.l. Elevations labeled "mnv" are m a.s.l. Scale 1:2500. GeoGIS [5], sketch 4.1.1.



Figure 6. Geodetic sketch of Ravne 3 on the 2026 orthophoto: 208.9 m, mean gradient 0.94%, entrance floor 470.04 m a.s.l. at the eastern portal, dry-stone walls marked. Scale 1:2500. GeoGIS [5], sketch 4.3.1.

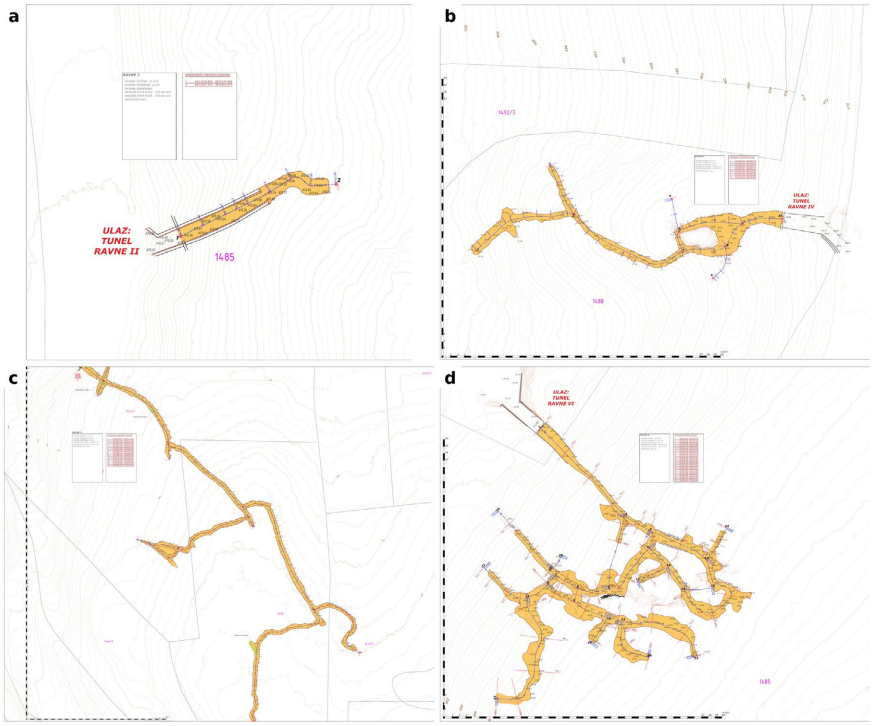


Figure 7. Geodetic sketches of (a) Ravne 2, 13.9 m, entrance at the western end; (b) Ravne 4, 84.4 m, mean gradient 1.9%; (c) Ravne 5, 251.3 m, 1.4%; and (d) Ravne 6, 187.7 m, 2.0%. Elevations labeled "mnv" are m a.s.l. Scale 1:2500. GeoGIS [5], sketches 4.2.1, 4.4.1, 4.5.1 and 4.6.1.

3.3. Floor Data

The point clouds themselves were not available for this study. GeoGIS supplied floor and ceiling points exported from them. The sketches are used only for the GeoGIS summary values in Table 2.

The floor points number 5191: Ravne 1, 2279; Ravne 2, 84; Ravne 3, 1526; Ravne 4, 273; Ravne 5, 666; and Ravne 6, 363. The entrance floor is the median of floor points within 2 m of the entrance point. The floor level at any other axis point is the median of points within 4 m. Points more than 0.5 m outward of the entrance point, and within 20 m of it, lie on the portal approach. These 75 points are excluded from floor ranges, gradients and end detection.

Mean floor gradients (Table 2) are those printed in the GeoGIS summary boxes. GeoGIS derived them from the point clouds. The sketches label the value "prosječni pad" (average fall). GeoGIS obtained it by joining the extreme points of the floor line on a longitudinal profile cut vertically along the main tunnel axis [17]. It is therefore an unsigned global slope of one profile. It ignores side branches and does not show which way the floor falls. We therefore computed a signed gradient from the floor points. Along-passage distance from the entrance was found as the shortest path through the floor and ceiling points, with links of 3 m or less. Floor points were grouped in 2 m distance bins, and the median height of each bin was regressed on distance. Each bin carries equal weight, so the gradient is length-

weighted and each branch counts in proportion to its length. A positive value means the floor rises away from the entrance. Bins of 1 - 5 m change the results by 0.25 percentage points or less.

GeoGIS notes that the points labeled floor include, in places, points on the gentle lower slopes toward the passage walls, recorded to model the full lower cross-section for volume calculation [17]. Such points sit above the floor proper and raise local maxima more than medians. As a check, we repeated the calculations with the lowest quartile of each bin instead of the median. Gradients stay positive in all six systems (0.24% - 2.76%), and Ravne 3 rises more steeply (0.70%). Floor maxima are the most affected values: the highest Ravne 3 point, 471.44 m, lies 0.44 m above the 99th percentile of that system.

3.4. Passage Ends and Orientation

A terminal end is an axis point whose floor points within 3 - 15 m lie mostly on one side (resultant length ≥ 0.75). The opposite direction is the way the passage end faces. The entrance is the axis point nearest the ULAZ label. An end faces a neighbor when the bearing to that system's nearest axis point, if within 300 m, lies within 35˚ of the end's facing direction.

To test whether facing ends are more common than chance, we kept every end at its surveyed position and gave it a random facing direction, uniform on 0˚ - 360˚. We repeated this 100000 times and counted facing ends in each run, following the logic of Monte Carlo significance tests for spatial pattern [19]. Azimuths were treated as circular data [20]. The p value is the share of runs at least as extreme as the observation; computing it as $(r + 1)/(n + 1)$ [21] changes no value at the precision reported. The same test was run at tolerances of 10˚, 15˚, and 20˚, for the mean angular offset to the nearest neighbor, and for mutually facing pairs of ends less than 100 m apart.

The uniform model treats every end as independent. Passage bearings within one system are not independent. They follow the layout of that system and may follow joints or bedding in the host rock. Two further null models keep this structure. In the rotation model, all ends of one system are rotated together by a single random angle, uniform on 0˚ - 360˚ and drawn separately for each system; relative bearings within the system are preserved. In the permutation model, the observed facing directions of each system are shuffled among that system's own ends, so each system keeps its observed set of directions. Each model was run 100,000 times with the same statistics as the uniform model.

3.5. Links and Valley Depth

For each pair of entrances and each candidate pair of facing ends we computed plan distance D, floor difference ΔH, and the gradient of a straight line between them, $S = \Delta H/D \times 100\%$. These straight lines are geometric possibilities, not reconstructed passage routes. Valley depth below tunnel level was read from GNSS control points on the valley floor.

3.6. Floor Surfaces

The surveyed floors are those exposed in 2026, after clearing that began in 2007. They are not proven excavation surfaces. Clearing removed backfill down to a firm surface of marl or conglomerate, and that surface was taken as the floor. Some backfill may remain on it, or clearing may have cut slightly into it; the scans cannot tell which.

Clearing and safety work have also changed the passages. Wheelbarrows used to remove backfill have worn shallow ruts into the floors. These are within the uncertainty of a floor level (Section 3.1), but they can form local hollows. Timber support, required by law for the safety of visitors, researchers and workers, has been installed along about 20% of the passage length. Passages about 1.5 m high were often enlarged to about 2 m to take the timber, and walls were sometimes widened. The extra height was gained by cutting the ceiling; floors were not lowered. Cross-sections in timbered sections are therefore modern, but their floor heights are not affected.

At all six entrances the ground in front of the portal has been paved, covered with a roof and lined with concrete walls. These works lie on the portal approaches, which are excluded from the analysis (Section 3.3). Only at Ravne 1 does the paving continue inside. Its first 8 m were paved: about 4 cm of clay was removed and 6 cm of concrete laid, so the floor there now stands about 0.02 m above the cleared surface. Two drainage channels run along the sides of this paved section. Floor points within it may fall on the channels, so the Ravne 1 entrance floor is the least certain of the six. Ravne 1 also has a modern service exit (Section 4.1). Interior floors in cleared, untimbered passages are taken as close to, but not certainly equal to, the original surface. All statements below about level, grading, planning and passage form refer to the present passages.

4. Results

4.1. Entrances and Floors at One Level

The six entrances lie between 470.04 and 471.50 m a.s.l., a spread of 1.46 m (**Table 2**, **Figure 8**). All interior floors lie between 469.93 and 475.50 m a.s.l. Beyond the Ravne 4 portal, the paved approach falls to 469.44 m within about 10 m; these points are excluded (Sections 3.3 and 3.6). At its south-western end (axis point 94; floor 473.10 m) Ravne 1 has a service exit into the park, dug by the Foundation. It is not an original entrance and is not used in the entrance comparison.

The survey points and the summary boxes disagree for four systems. Of 653 interior Ravne 5 points, 369 exceed the 471.33 m maximum printed in its summary box; of 354 Ravne 6 points, 76 exceed 472.72 m. The Ravne 2 and Ravne 3 maxima are exceeded by up to 0.25 m and 0.46 m. This study uses the survey points. All other values agree within 0.08 m.

4.2. Floors Rise Away from the Entrances

All six entrance floors lie within 0.11 m of the lowest recorded floor of their system. With the lowest quartile of nearby points instead of the median, the figure

falls to 0.09 m (Section 3.3). Each entrance is therefore at or near the lowest point of its system. GeoGIS reports mean gradients of 0.94% - 2.0% for five systems; these are unsigned (Section 3.3) and do not on their own show direction. No mean gradient is reported for the 13.9 m Ravne 2. Inner floors rise 0.4 - 4.0 m above the entrances: 4.0 m in Ravne 1, 2.4 m in Ravne 5, 2.2 m in Ravne 6, 1.5 m in Ravne 4, 1.4 m in Ravne 3, and 0.4 m in Ravne 2. Signed gradients from the floor points are positive in all six systems (Table 2): 0.23% in Ravne 1, 0.84% in Ravne 2, 0.49% in Ravne 3, 2.71% in Ravne 4, 1.61% in Ravne 5 and 2.12% in Ravne 6. No 2 m distance bin lies more than 0.05 m below its entrance floor. The rise is not uniform. Ravne 3 and Ravne 6 gain most of their height within about 15 m of the portal; beyond 10 m, Ravne 3 is close to level (−0.27%) and Ravne 6 rises at 0.92%. The GeoGIS values are close to the signed gradients only in Ravne 5 and Ravne 6. Neither result proves a continuous fall along every branch, and local hollows that would hold water are not excluded.

Table 2. Entrances and floor levels of the six systems. Entrance floors are medians of floor points within 2 m of the entrance point. Floor ranges are taken from interior floor points, portal approaches excluded; the summary box on each sketch is given for comparison. Mean gradient: GeoGIS summary value/signed gradient from the floor points (Section 3.3; positive values rise away from the entrance).

System	Entrance Y (m)	Entrance X (m)	Entrance floor (m a.s.l.)	Floor range, survey points (m a.s.l.)	Floor range, sketch summary (m a.s.l.)	Length (m)	Mean gradient, GeoGIS/signed (%)
Ravne 1	6513219.88	4872433.48	471.50	471.42 - 475.50	471.50 - 475.50	1706.5	1.0/+0.23
Ravne 2	6513154.86	4872157.67	470.48	470.44 - 470.90	470.44 - 470.65	13.9	—/+0.84
Ravne 3	6513038.19	4872407.73	470.04	469.93 - 471.44	469.95 - 470.98	208.9	0.94/+0.49
Ravne 4	6512943.43	4872101.57	470.52	470.45 - 472.00	470.45 - 472.00	84.4	1.9/+2.71
Ravne 5	6513259.01	4872616.66	470.11	470.11 - 472.49	470.05 - 471.33	251.3	1.4/+1.61
Ravne 6	6513013.97	4872138.12	471.33	471.33 - 473.50	471.33 - 472.72	187.7	2.0/+2.12
Total			470.04 - 471.50	469.93 - 475.50	469.95 - 475.50	2452.7	

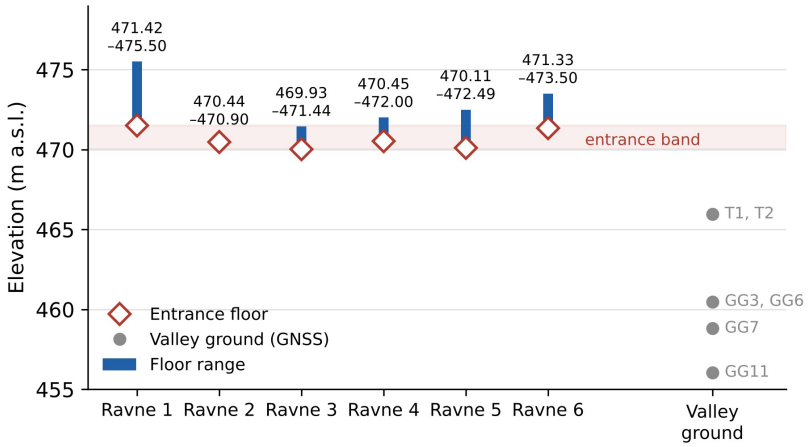


Figure 8. Floor range of each system from survey floor points (bars), entrance floor (diamonds) and valley ground at GNSS control points (dots). Shaded band: entrance level, 470.04 - 471.50 m a.s.l.

4.3. Entrance-to-Entrance Distances

Any two entrances could be joined by a straight line at 1.02% or less (Table 3). These lines are mathematical possibilities, not established routes. The Ravne 3 portal opens at 84˚, within 2˚ of the bearing to the Ravne 1 portal across the valley. The Ravne 4 portal opens at 73˚, within 11˚ of the bearing to the Ravne 6 portal and within 3˚ of the bearing to Ravne 6 axis point 23 (L3, Table 4).

Table 3. Entrance pairs, sorted by distance.

Pair	D (m)	ΔH (m)	S (%)
Ravne 4 - Ravne 6	79.4	0.81	1.02
Ravne 2 - Ravne 6	142.2	0.85	0.60
Ravne 1 - Ravne 3	183.5	1.46	0.80
Ravne 1 - Ravne 5	187.3	1.39	0.74
Ravne 2 - Ravne 4	218.7	0.04	0.02
Ravne 3 - Ravne 6	270.7	1.29	0.48
Ravne 2 - Ravne 3	275.9	0.44	0.16
Ravne 1 - Ravne 2	283.4	1.02	0.36
Ravne 3 - Ravne 5	304.0	0.07	0.02
Ravne 3 - Ravne 4	320.5	0.48	0.15
Ravne 1 - Ravne 6	360.1	0.17	0.05
Ravne 1 - Ravne 4	432.0	0.98	0.23
Ravne 2 - Ravne 5	470.7	0.37	0.08
Ravne 5 - Ravne 6	537.6	1.22	0.23
Ravne 4 - Ravne 5	604.1	0.41	0.07

4.4. Passage Orientation Is Not Distinguishable from Chance

The six systems have 45 terminal ends, 21 of them in Ravne 1. Of these, 20 point within 35˚ at a neighboring system less than 300 m away. Random orientations give 19.0 ± 3.1 facing ends, and 44% of random runs give 20 or more ($p = 0.44$). Tighter tolerances give the same answer: 5 ends within 10˚ (random mean 6.4; $p = 0.79$), 7 within 15˚ (9.2; $p = 0.85$), and 11 within 20˚ (11.9; $p = 0.68$). The mean offset to the nearest neighbor is 61˚ (random mean 57˚; $p = 0.75$). Excluding Ravne 1, 10 of 24 ends face a neighbor (random mean 10.5; $p = 0.67$). Mutually facing pairs less than 100 m apart number two: L1, between Ravne 1 and Ravne 5, and L3, between the Ravne 4 portal and Ravne 6. Random orientations give two or more such pairs in 17% of runs and at least one in 45%.

The two structure-preserving null models give the same answer. Under the rotation model, random runs give 19.0 ± 2.0 facing ends at 35˚ ($p = 0.41$); under the permutation model, 18.1 ± 1.9 ($p = 0.23$). At tolerances of 10˚ - 20˚, p ranges from 0.71 to 0.88 under rotation and from 0.92 to 0.97 under permutation. Two or more mutually facing pairs occurred in 16% and 27% of runs. Keeping each system's

own directional pattern does not reveal an excess of facing ends.

As a group, the passage ends do not point at neighboring systems more often than chance. This prediction of H1 is not supported. Individual alignments remain worth testing, because chance alignment and a real link cannot be told apart from orientation alone. Table 4 lists the candidate pairs, separating the mutual pairs from one-sided alignments (Figure 9).

Table 4. Candidate links between facing ends, as priority targets for geophysics. Alignment is the angle between the direction an end faces and the bearing to the other system. D is given to the nearest meter, and ΔH and S to 0.1, to reflect the uncertainty of the floor levels and of the end positions.

Link	Type	From (system, axis point, floor m)	To (system, axis point, floor m)	D (m)	ΔH (m)	S (%)	Alignment
L1	Mutual	Ravne 1, pt 35, 472.6	Ravne 5, pt 15, 472.2	50	0.4	0.7	27˚ and 15˚
L2	One-sided	Ravne 5, pt 14, 472.3	Ravne 1, pt 37, 472.6	64	0.3	0.4	Ravne 5 end, 28˚
L3	Mutual	Ravne 4 entrance, 470.5	Ravne 6, pt 23, 472.6	64	2.1	3.3	3˚ and 32˚
L4	Mutual, >100 m	Ravne 6, pt 24, 473.2	Ravne 1 SW end, pt 94, 473.1	174	0.2	0.1	5˚ and 30˚
L5	One-sided	Ravne 3 entrance, 470.0	Ravne 1 entrance, 471.5	184	1.5	0.8	Ravne 3 portal, 2˚
L6	One-sided	Ravne 6, pt 24, 473.2	Ravne 1, pt 97, 473.5	222	0.3	0.1	Ravne 6 end, 31˚
L7	One-sided	Ravne 3, pt 24, 470.6	Ravne 2 entrance, 470.5	253	0.1	<0.1	Ravne 3 end, 15˚

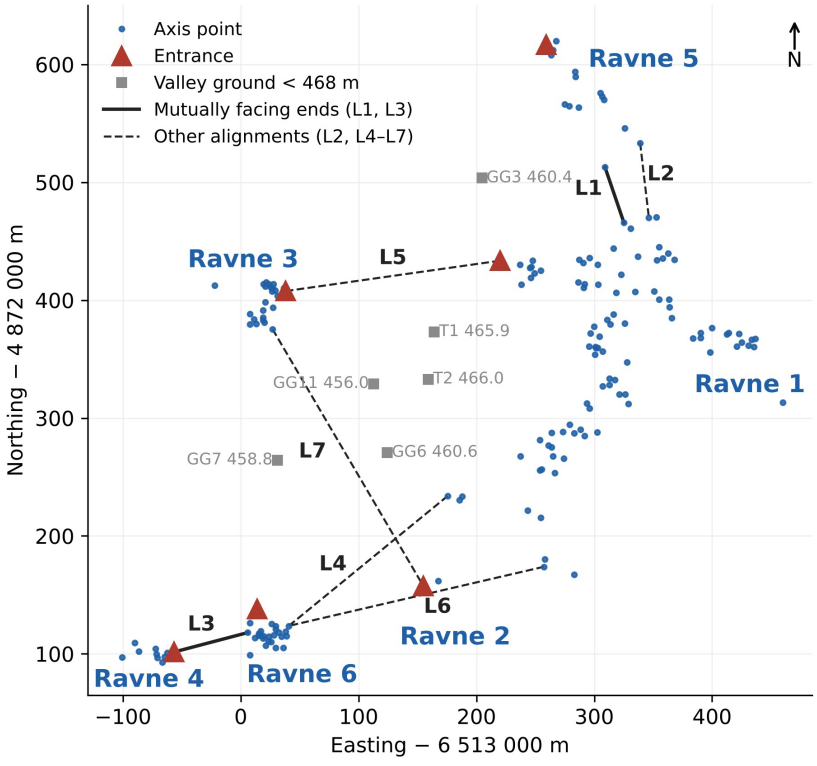


Figure 9. Plan of the six systems from the 2026 survey: axis points, entrances, valley control points below 468 m a.s.l. and candidate links L1 - L7. Solid lines: mutually facing ends less than 100 m apart (L1, L3); dashed lines: other alignments. Straight lines are geometric possibilities, not reconstructed routes. MGI/Balkans zone 6.

4.5. The Valley below Tunnel Level

The floor of Park Ravne 2 lies 4 - 19 m below tunnel level (Figure 10). Valley control points read 456.05 m (GG11), 458.81 m (GG7), 460.41 m (GG3), 460.56 m (GG6), and 465.95 - 465.96 m a.s.l. (T1, T2). T1 lies 4.1 m below the Ravne 3 entrance floor. GG6 lies 31 m from line L7 and 10.0 m below it. GG7, between Ravne 3 and Ravne 6, lies 11.2 m below the Ravne 3 entrance floor.

Lines L4 - L7 cross the valley; L1 - L3 stay within one slope. GG5 lies 6 m from line L6 and 3.0 m below it. A passage at the level of L4 - L7 would have run through ground that is no longer present. East of the valley the hill rises to 493.5 - 500.2 m a.s.l. (GG12 - GG15), giving about 18 - 29 m of cover over Ravne 1. Figure 10 combines points from different northings; it shows depth below tunnel level, not the form of the valley.

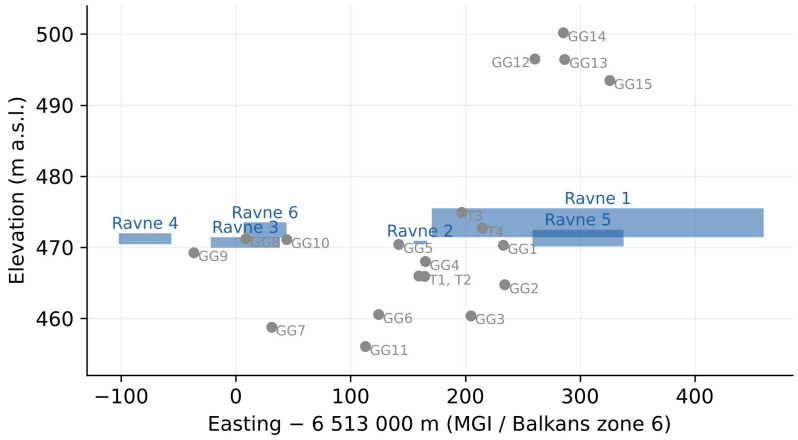


Figure 10. Composite east-west elevation diagram. Bars: floor range of each system across its easting extent. Dots: GNSS control points, drawn from different northings, so the diagram is not a true section.

5. Discussion

5.1. What the Data Show

Two results stand. First, all portals lie within 1.46 m and all floors within 5.6 m, over 0.6 km and six separate systems. Second, each entrance lies within 0.11 m of the lowest floor of its system, inner floors rise 0.4 - 4.0 m above it, and signed gradients are positive in all six systems. The restricted range of entrance elevations is consistent with coordinated vertical planning, if the present floors approximate the original ones (Section 3.6), but cannot independently distinguish a formerly connected network from separate excavations exploiting a common geological or topographic level.

The third line of evidence tested here, passage orientation, does not favor H1. Facing ends occur at the rate expected from random orientations. Two or more mutually facing pairs occurred in 17% of null simulations under the uniform model, and in 16% and 27% under the structure-preserving models. That figure concerns the dataset as a whole. It does not test L1 itself, its 50 m separation, or its 0.4 m

floor difference. L1 is the best target for a direct test, not evidence of a link. The second pair, L3, faces across a 2.1 m difference in floor level, which a link would have to climb at 3.3%.

The archaeology shows that passages once ran further than they do now. Five systems end in backfill and dry-stone closures, not in rock (Figure 11). Where those passages led is the open question.

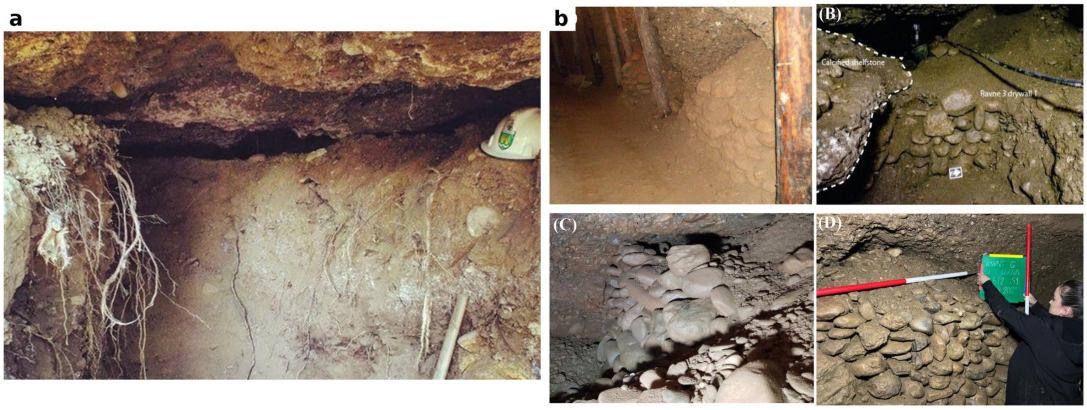


Figure 11. (a) Entrance zone of a rubble-filled passage in Ravne 3, between a conglomerate ceiling and a marl floor [9]. (b) Dry-stone constructions within the Ravne underground complex ([2], CC BY 4.0).

5.2. Weighing the Hypotheses

H3 accounts for the portal level and the outward grading as well as H1 does. If the valley already existed, separate adits driven into both flanks from one working level would open at one height and drain outward. H3 also predicts that passage ends show no preferred direction toward neighbors, which is what the Monte Carlo test found. On the present evidence H3 fits at least as well as H1.

H2 cannot be tested with the present data. A tunnel driven along a near-horizontal contact keeps a near-constant level whoever dug it. The Ravne 3 passage with a conglomerate ceiling and a marl floor fits this reading (Figure 3; Figure 11(a)). The decisive measurement is the elevation of the unconformity where passages cross it. If floors stay at 470 - 472 m where the contact rises or falls, H2 is rejected. If they follow it, H2 explains the common level without a network. The Miocene beds dip north-west, but the erosional surface on them need not follow that dip, so it must be mapped inside the tunnels.

The recurrence of comparable passage morphology in unmodified sections, river-pebble dry-stone closures, and anthropogenic backfilling across multiple Ravne systems provides archaeological evidence of shared construction and closure practices. Although these similarities cannot establish physical connectivity, they warrant consideration alongside the geodetic relationships. They are also compatible with separate systems built within one tradition.

5.3. The Valley and the Chronology

A valley floor 4 - 19 m below tunnel level does not show that the valley post-dates

the tunnels. It shows only that any link across it is now missing. The test is geological: whether sediments and erosional surfaces in the valley record removal of rock that once joined the two slopes, and when. Late Pleistocene floods, gradual fluvial incision, and slope retreat are all possible mechanisms. Climatically driven incision and terrace formation are widespread in Quaternary river valleys [22] [23], so the Ravne valley could predate or postdate the tunnels. Dated valley-floor deposits and a bare-earth LiDAR profile, interpreted with terrain-visualization methods such as openness [15], are needed to choose between them.

The Ravne 3 stalagmites stand on passage floors inside the system. If they grew *in situ* on undisturbed floors, those passages were open and stable by 19,000 ± 1000 years BP. This is a minimum age for those passages only. It does not show that the whole of Ravne 3, or the other systems, existed then, and it does not date the valley.

Lines L1, L2, and L3 do not cross the valley. If a buried passage is found along any of them, H1 holds for those two systems whatever the age of the valley.

5.4. Limitations

- Floor levels come from GeoGIS point lists, not from the point clouds themselves. Some points lie on the lower side slopes, and scan-chain closure residuals are not reported (Sections 3.1 and 3.3). **Table 4** gives D to the nearest meter and ΔH and S to 0.1.
- Each tunnel is tied to the common frame through the LiDAR cloud around its entrance, with small overlaps. Inter-system height differences below about 0.3 m are therefore not resolved (Section 3.1).
- Measured floors are cleared surfaces, rutted by wheelbarrow traffic and, over the first 8 m of the Ravne 1 entrance, paved and flanked by drainage channels (Section 3.6). About 20% of passage length has been enlarged for timber support by cutting the ceiling, so cross-sections there are modern (**Figure 12**). Correspondence of the present floors to the original excavation floors is not established.
- The sketch summary maxima for Ravne 2, 3, 5 and 6 are exceeded by the survey points. GeoGIS attributes such differences to summary values taken over a different extent and set of point classes than the sketch heights [17]. The analysis uses the survey points throughout.
- The GeoGIS mean gradients are unsigned slopes of a single axial profile (Section 3.3); grading toward the portals rests on the signed gradients computed here.
- Terminal ends are found by a geometric rule, not from field logs; some may be junctions or alcoves. Misclassified ends would add noise to the orientation test.
- The Ravne 1 end in L4 now carries a service exit dug by the Foundation; L4 tests the alignment of the two passage ends, not an original opening.
- No in-tunnel elevations of the conglomerate-marl contact were available, so H2 could not be tested.
- Valley control points are sparse; the nearest to a valley-crossing line lies 31 m

from it (GG6, L7); no bare-earth valley profile was available.

- Backfilled, flooded, and very low sections were not scanned, and no dated sediment from the valley floor is yet available.



(a) (b)

Figure 12. Modern modification of the passages. (a) Installation of timber support; passages were enlarged by cutting the ceiling to take the frames. (b) Clearing of backfill by wheelbarrow, which wears shallow ruts into the floor. Foundation photographs, 2026.

6. Conclusions

The 2026 geodetic dataset identifies a series of spatially and vertically compatible relationships among the six Ravne tunnel systems. All entrances lie at 470.04 - 471.50 m a.s.l., each entrance lies within 0.11 m of its system's lowest present floor, and floors rise away from all six portals. Passage ends do not point at neighboring systems more often than chance, but one pair, the closely spaced, mutually facing ends of Ravne 1 and Ravne 5, justifies targeted investigation of a possible former connection. The available evidence does not yet distinguish conclusively between a formerly integrated underground network, separate excavations developed along a common geological horizon, and independently constructed passages originating from an existing valley. Four tests can resolve these alternatives:

1) GPR or electrical resistivity tomography between the facing ends of L1 and L2 (about 50 - 64 m apart, on the same slope). A buried passage there would establish a former link between Ravne 1 and Ravne 5 without reference to the valley.

2) Elevations of the conglomerate-marl unconformity where it is exposed inside the tunnels, compared with floor levels.

3) Classification of each terminal end from field logs as backfilled, walled, or rock-bound, and a repeat of the orientation test on backfilled ends only.

4) Bare-earth LiDAR profiles and dated sediments along L5 and L7, to measure and date the ground missing between the slopes.

Data Availability

Axis coordinates, control points, and geodetic sketches are in the GeoGIS deliverables (lists 5.1 and 5.2.1 - 5.2.6; sketches 4.1.1 - 4.6.2; September 2026), held by the Foundation and available on request. Derived entrance and end levels are given in Tables 2-4. The 45 terminal ends with coordinates, floor levels, and facing directions (S1), the axis points (S2), the GeoGIS floor and ceiling point lists (S3), and the analysis script with its three null models (S4) are provided as Supplementary Materials.

Acknowledgements

The author thanks GeoGIS studio d.o.o. Sarajevo for the 2026 survey. GeoGIS staff shown in Figure 4 consented to publication of the photographs.

Conflicts of Interest

The author leads the foundation that manages the Ravne site and commissioned the survey.

References

[1] Osmanagich, S. (2025) A New Class of Subterranean Dry-Stone Structures: River-Pebble Walls in the Ravne Tunnel Complex, Bosnia-Herzegovina. *Journal of Environment and Biological Science*, **1**, 1-14. https://doi.org/10.64142/jebs.1.1.5

[2] Osmanagich, S. (2026) Systematic Archaeological Investigation of the Ravne Underground Complex in Bosnia and Herzegovina. *Archaeological Discovery*, **14**, 125-151. https://doi.org/10.4236/ad.2026.142007

[3] Osmanagich, S. (2026) Deliberate Closure of Constructed Spaces: An Anthropological Analysis of Backfilling and Sealing in the Ravne Tunnel System (Bosnia and Herzegovina) and Göbekli Tepe (Turkey). *Global Journal of Human-Social Science*, **26**, 1-10. https://doi.org/10.34257/gjhssd257126

[4] Šabanija-Softić, A. and Osmanagich, S. (2026) Archaeological Excavation of the Ravne 6 Tunnel (Visoko, Bosnia and Herzegovina): Results from the 2025 Field Season. *Archaeological Discovery*, **14**, 171-188. https://doi.org/10.4236/ad.2026.142009

[5] GeoGIS Studio (2026) Tehnički izvještaj: Geodetsko snimanje, lasersko skeniranje i LiDAR snimanje kompleksa Ravne u Visokom [Technical Report: Geodetic Survey, Laser Scanning and LiDAR Survey of the Ravne Complex in Visoko]. GeoGIS Studio, Sarajevo. Unpublished Technical Report to the Archaeological Park: Bosnian Pyramid of the Sun Foundation, Visoko; Available from the Foundation on Request.

[6] Osmanagich, S. (2026) Integrated 3D Laser Scanning, LiDAR and GIS Documentation of the Ravne Underground Complex (Bosnia and Herzegovina): Spatial Architecture of Six Tunnel Systems. *Journal of Geographic Information System*, **18**, No. 6. (In Press)

[7] Schmid, S.M., Bernoulli, D., Fügenschuh, B., Matenco, L., Schefer, S., Schuster, R., *et al.* (2008) The Alpine-Carpathian-Dinaridic Orogenic System: Correlation and Evolution of Tectonic Units. *Swiss Journal of Geosciences*, **101**, 139-183. https://doi.org/10.1007/s00015-008-1247-3

[8] de Leeuw, A., Mandic, O., Krijgsman, W., Kuiper, K. and Hrvatović, H. (2012) Pale-

omagnetic and Geochronologic Constraints on the Geodynamic Evolution of the Central Dinarides. *Tectonophysics*, **530**, 286-298. https://doi.org/10.1016/j.tecto.2012.01.004

[9] Osmanagich, S. (2025) Archaeological Stratigraphy and Environmental Analysis of the Ravne 3 Tunnel Complex (Visoko, Bosnia-Herzegovina): Evidence from Multi-Period Artifacts, Radiometric Dating, and Energetic Microclimate Data. *Acta Scientific Environmental Science*, **2**, 68-96. https://actascientific.com/ASES/pdf/ASES-02-0011.pdf

[10] Osmanagich, S. (2025) Establishing Deep Time: Multi-Method Dating of Archaeological and Speleological Features in the Bosnian Valley of the Pyramids. *Geoinformatics & Geostatistics*: *An Overview*, **13**, 1-12.

[11] Richards, D.A. and Dorale, J.A. (2003) Uranium-Series Chronology and Environmental Applications of Speleothems. *Reviews in Mineralogy and Geochemistry*, **52**, 407-460. https://doi.org/10.2113/0520407

[12] Fairchild, I.J. and Baker, A. (2012) Speleothem Science: From Process to Past Environments. Wiley. https://doi.org/10.1002/9781444361094

[13] Fekete, S., Diederichs, M. and Lato, M. (2010) Geotechnical and Operational Applications for 3-Dimensional Laser Scanning in Drill and Blast Tunnels. *Tunnelling and Underground Space Technology*, **25**, 614-628. https://doi.org/10.1016/j.tust.2010.04.008

[14] Chase, A.F., Chase, D.Z., Weishampel, J.F., Drake, J.B., Shrestha, R.L., Slatton, K.C., *et al*. (2011) Airborne LiDAR, Archaeology, and the Ancient Maya Landscape at Caracol, Belize. *Journal of Archaeological Science*, **38**, 387-398. https://doi.org/10.1016/j.jas.2010.09.018

[15] Doneus, M. (2013) Openness as Visualization Technique for Interpretative Mapping of Airborne Lidar Derived Digital Terrain Models. *Remote Sensing*, **5**, 6427-6442. https://doi.org/10.3390/rs5126427

[16] Osmanagich, S. (2026) An Anthropological Interpretation of the Subterranean Ravne Tunnel System (Central Bosnia). *Advances in Anthropology*, **16**, 23-50. https://doi.org/10.4236/aa.2026.161002

[17] Žutić, A. (2026) Rekapitulacija tehničkog izvještaja: Geodetsko snimanje, GNSS kontrolna osnova, UAV LiDAR i 3D lasersko skeniranje tunela Ravne 1-6 [Recapitulation of the Technical Report: Geodetic Survey, GNSS Control, UAV LiDAR and 3D Laser Scanning of Tunnels Ravne 1-6]. GeoGIS Studio, Sarajevo. Unpublished Supplement to the Technical Report [5]; Available from the Foundation on Request.

[18] Ključanin, S. and Redžepagić, E. (2021) Introduction of the New Geodetic Datums and Map Projections in the Federation of Bosnia and Herzegovina. *E-Zbornik*, *elektronički zbornik radova Građevinskog fakulteta*, **11**, 62-77. https://doi.org/10.47960/2232-9080.2021.22.11.62

[19] Besag, J. and Diggle, P.J. (1977) Simple Monte Carlo Tests for Spatial Pattern. *Applied Statistics*, **26**, 327-333. https://doi.org/10.2307/2346974

[20] Fisher, N.I. (1993) Statistical Analysis of Circular Data. Cambridge University Press. https://doi.org/10.1017/cbo9780511564345

[21] North, B.V., Curtis, D. and Sham, P.C. (2002) A Note on the Calculation of Empirical P Values from Monte Carlo Procedures. *The American Journal of Human Genetics*, **71**, 439-441. https://doi.org/10.1086/341527

[22] Bridgland, D. and Westaway, R. (2008) Climatically Controlled River Terrace Staircases: A Worldwide Quaternary Phenomenon. *Geomorphology*, **98**, 285-315.

https://doi.org/10.1016/j.geomorph.2006.12.032

[23] Vandenberghe, J. (2015) River Terraces as a Response to Climatic Forcing: Formation Processes, Sedimentary Characteristics and Sites for Human Occupation. *Quaternary International*, **370**, 3-11. https://doi.org/10.1016/j.quaint.2014.05.046

Supplementary Materials

Contents

- **S1.** Terminal passage ends (Table S1, 45 records).
- **S2.** Tunnel axis points with floor levels (Table S2, 175 records).
- **S3.** Surveyor's floor, ceiling and axis point lists (inventory in Table S3; data files supplied separately).
- **S4.** Analysis script (Python listing).

Coordinate and height reference

All coordinates are in the state coordinate system of Bosnia and Herzegovina: Gauss-Krüger projection, zone 6 (central meridian 18° E), Bessel 1841 ellipsoid (MGI/Balkans zone 6). Y is easting and X is northing, in metres. Heights (H) are in metres in the height system BH_VRS1971.5, as stated by the surveyor (GeoGIS studio, Sarajevo; project 171_26_LIDAR_GEO).

S1. Terminal Passage Ends

Table S1 lists the 45 axis points classified as terminal passage ends. For each axis point, unit vectors were drawn to all interior floor points at 3 - 15 m distance. A point was classed as a terminal end when the mean resultant length of these vectors was 0.75 or more. The facing direction is the bearing opposite to the mean vector, *i.e.*, the direction in which the passage ends. Bearings are clockwise from grid north. Five of the ends are tunnel entrances.

Table S1. Terminal passage ends of the six Ravne tunnel systems.

System	Axis point	Y (easting), m	X (northing), m	Floor level, m	Facing, °	Resultant length	Entrance
Ravne 1	3	6513238.063	4872413.139	472.664	228.5	0.809	no
Ravne 1	8	6513247.816	4872433.501	472.572	19.8	0.832	no
Ravne 1	14	6513286.961	4872434.397	472.767	282.9	0.859	no
Ravne 1	28	6513325.786	4872380.236	472.735	117.7	0.778	no
Ravne 1	29	6513295.696	4872360.873	473.079	249.8	0.830	no
Ravne 1	32	6513300.576	4872353.955	473.016	195.0	0.907	no
Ravne 1	35	6513325.101	4872465.899	472.570	313.7	0.759	no
Ravne 1	37	6513346.344	4872469.829	472.566	33.2	0.778	no
Ravne 1	38	6513352.731	4872470.443	—	54.9	0.922	no
Ravne 1	41	6513367.954	4872434.201	473.273	110.2	0.772	no
Ravne 1	49	6513365.823	4872384.810	473.127	195.8	0.792	no
Ravne 1	51	6513383.768	4872367.626	472.877	231.1	0.810	no
Ravne 1	53	6513398.404	4872355.612	473.067	168.3	0.978	no
Ravne 1	62	6513436.452	4872367.256	474.380	47.1	0.832	no
Ravne 1	64	6513459.949	4872313.099	475.226	132.5	0.999	no
Ravne 1	73	6513295.924	4872308.267	473.617	118.9	0.902	no

Continued

Ravne 1	80	6513302.419	4872288.055	473.186	95.2	0.989	no
Ravne 1	87	6513237.340	4872267.778	472.766	322.5	1.000	no
Ravne 1	94	6513175.635	4872233.946	473.096	261.0	0.759	no
Ravne 1	97	6513257.269	4872173.869	473.541	216.0	0.838	no
Ravne 1	98	6513282.882	4872167.232	473.950	122.8	0.998	no
Ravne 2	1	6513154.855	4872157.665	470.476	246.0	0.997	yes
Ravne 2	2	6513167.423	4872161.874	470.631	79.5	0.989	no
Ravne 3	1	6512977.798	4872412.476	470.584	269.3	0.986	no
Ravne 3	4	6513021.521	4872415.331	470.904	336.0	0.791	no
Ravne 3	11	6513036.352	4872410.023	470.755	69.4	0.849	no
Ravne 3	12	6513038.193	4872407.731	470.035	84.3	0.871	yes
Ravne 3	18	6513007.619	4872388.329	470.695	299.9	0.942	no
Ravne 3	20	6513007.570	4872379.549	470.739	243.6	0.906	no
Ravne 3	24	6513026.955	4872375.399	470.564	134.9	0.943	no
Ravne 4	1	6512899.160	4872096.977	471.666	238.0	0.983	no
Ravne 4	3	6512909.878	4872109.218	471.393	356.2	0.870	no
Ravne 4	10	6512943.429	4872101.566	470.519	72.5	0.972	yes
Ravne 5	1	6513259.014	4872616.664	470.112	299.1	0.945	yes
Ravne 5	3	6513263.369	4872607.909	470.222	211.7	0.782	no
Ravne 5	4	6513267.618	4872619.950	470.343	16.5	0.885	no
Ravne 5	11	6513278.533	4872564.821	471.684	283.4	0.965	no
Ravne 5	12	6513275.063	4872566.067	471.693	287.6	0.989	no
Ravne 5	14	6513338.900	4872533.428	472.299	145.3	0.951	no
Ravne 5	15	6513309.110	4872512.750	472.219	176.3	0.995	no
Ravne 6	1	6513013.974	4872138.124	471.333	321.0	0.932	yes
Ravne 6	12	6513036.100	4872105.032	472.735	157.4	0.772	no
Ravne 6	22	6513007.583	4872099.079	472.786	224.5	0.928	no
Ravne 6	23	6513005.802	4872117.987	472.630	287.4	0.858	no
Ravne 6	24	6513040.766	4872123.703	473.248	46.1	0.850	no

— No floor level: no surveyed floor point lies within 4 m of Ravne 1 axis point 38 (nearest at 5.5 m).

S2. Tunnel Axis Points

Table S2 lists the 175 passage axis points from the surveyor's axis files (S3). The floor level is the median height of the surveyed floor points within 4 m of the axis point, excluding points on the entrance approach.

Table S2. Axis points of the six Ravne tunnel systems.

System	Axis point	Y (easting), m	X (northing), m	Floor level, m
Ravne 1	1	6513219.882	4872433.481	471.500
Ravne 1	2	6513237.072	4872429.954	472.386
Ravne 1	3	6513238.063	4872413.139	472.664
Ravne 1	4	6513246.016	4872418.836	472.557
Ravne 1	5	6513249.113	4872422.870	472.448
Ravne 1	6	6513245.418	4872427.475	472.512
Ravne 1	7	6513246.466	4872428.121	472.520
Ravne 1	8	6513247.816	4872433.501	472.572
Ravne 1	9	6513254.432	4872424.986	472.875
Ravne 1	10	6513286.436	4872415.347	472.852
Ravne 1	11	6513291.160	4872410.575	472.966
Ravne 1	12	6513291.836	4872413.804	472.980
Ravne 1	13	6513290.745	4872431.812	472.693
Ravne 1	14	6513286.961	4872434.397	472.767
Ravne 1	15	6513295.897	4872436.059	472.726
Ravne 1	16	6513302.847	4872430.240	472.928
Ravne 1	17	6513316.455	4872443.892	472.709
Ravne 1	18	6513336.788	4872437.153	472.814
Ravne 1	19	6513322.953	4872421.627	473.133
Ravne 1	20	6513303.072	4872413.267	473.036
Ravne 1	21	6513318.406	4872406.549	472.989
Ravne 1	22	6513316.126	4872388.155	472.841
Ravne 1	23	6513311.019	4872383.212	472.920
Ravne 1	24	6513299.667	4872377.776	473.142
Ravne 1	25	6513296.814	4872371.980	473.037
Ravne 1	26	6513304.291	4872369.172	473.058
Ravne 1	27	6513313.697	4872379.647	472.928
Ravne 1	28	6513325.786	4872380.236	472.735
Ravne 1	29	6513295.696	4872360.873	473.079
Ravne 1	30	6513300.913	4872360.201	473.089
Ravne 1	31	6513301.372	4872359.687	473.085
Ravne 1	32	6513300.576	4872353.955	473.016
Ravne 1	33	6513302.754	4872359.675	473.082
Ravne 1	34	6513306.917	4872356.517	472.978
Ravne 1	35	6513325.101	4872465.899	472.570

Continued

Ravne 1	36	6513330.923	4872460.864	472.581
Ravne 1	37	6513346.344	4872469.829	472.566
Ravne 1	38	6513352.731	4872470.443	—
Ravne 1	39	6513355.052	4872445.035	472.724
Ravne 1	40	6513362.552	4872439.632	473.069
Ravne 1	41	6513367.954	4872434.201	473.273
Ravne 1	42	6513353.192	4872433.940	473.244
Ravne 1	43	6513358.072	4872435.554	473.032
Ravne 1	44	6513350.711	4872407.667	473.344
Ravne 1	45	6513354.976	4872400.744	473.406
Ravne 1	46	6513363.467	4872400.679	473.767
Ravne 1	47	6513334.510	4872407.268	473.103
Ravne 1	48	6513363.671	4872394.279	473.115
Ravne 1	49	6513365.823	4872384.810	473.127
Ravne 1	50	6513390.179	4872372.430	473.291
Ravne 1	51	6513383.768	4872367.626	472.877
Ravne 1	52	6513390.206	4872368.226	472.979
Ravne 1	53	6513398.404	4872355.612	473.067
Ravne 1	54	6513412.320	4872370.962	473.829
Ravne 1	55	6513399.691	4872376.491	473.408
Ravne 1	56	6513414.110	4872372.449	473.833
Ravne 1	57	6513422.758	4872371.567	472.851
Ravne 1	58	6513424.990	4872364.147	—
Ravne 1	59	6513420.963	4872360.861	473.783
Ravne 1	60	6513430.949	4872361.438	474.009
Ravne 1	61	6513433.478	4872366.552	474.291
Ravne 1	62	6513436.452	4872367.256	474.380
Ravne 1	63	6513435.416	4872360.200	474.317
Ravne 1	64	6513459.949	4872313.099	475.226
Ravne 1	65	6513317.469	4872332.515	472.853
Ravne 1	66	6513327.714	4872347.473	472.804
Ravne 1	67	6513321.347	4872320.296	473.470
Ravne 1	68	6513326.176	4872320.249	473.036
Ravne 1	69	6513312.950	4872328.247	472.899
Ravne 1	70	6513312.948	4872333.479	472.900
Ravne 1	71	6513306.981	4872327.143	473.230
Ravne 1	72	6513329.091	4872312.206	472.980

Continued

Ravne 1	73	6513295.924	4872308.267	473.617
Ravne 1	74	6513293.572	4872312.382	473.571
Ravne 1	75	6513279.000	4872294.637	473.431
Ravne 1	76	6513273.374	4872288.399	473.488
Ravne 1	77	6513283.053	4872287.111	473.302
Ravne 1	78	6513291.657	4872284.951	473.269
Ravne 1	79	6513288.236	4872290.135	473.226
Ravne 1	80	6513302.419	4872288.055	473.186
Ravne 1	81	6513274.218	4872265.666	473.326
Ravne 1	82	6513264.969	4872267.526	473.550
Ravne 1	83	6513263.665	4872275.361	473.380
Ravne 1	84	6513261.046	4872276.912	473.461
Ravne 1	85	6513253.757	4872281.411	473.837
Ravne 1	86	6513263.897	4872287.511	473.845
Ravne 1	87	6513237.340	4872267.778	472.766
Ravne 1	88	6513253.636	4872255.635	473.594
Ravne 1	89	6513255.334	4872256.405	473.577
Ravne 1	90	6513266.474	4872253.450	473.151
Ravne 1	91	6513243.401	4872221.599	473.923
Ravne 1	92	6513254.375	4872215.437	473.609
Ravne 1	93	6513258.091	4872180.241	473.424
Ravne 1	94	6513175.635	4872233.946	473.096
Ravne 1	95	6513187.807	4872233.680	473.151
Ravne 1	96	6513185.734	4872230.314	473.151
Ravne 1	97	6513257.269	4872173.869	473.541
Ravne 1	98	6513282.882	4872167.232	473.950
Ravne 2	1	6513154.855	4872157.665	470.476
Ravne 2	2	6513167.423	4872161.874	470.631
Ravne 3	1	6512977.798	4872412.476	470.584
Ravne 3	2	6513019.423	4872413.493	470.914
Ravne 3	3	6513020.849	4872411.899	470.911
Ravne 3	4	6513021.521	4872415.331	470.904
Ravne 3	5	6513024.021	4872413.490	470.906
Ravne 3	6	6513027.523	4872413.560	470.896
Ravne 3	7	6513025.430	4872411.017	470.908
Ravne 3	8	6513026.655	4872407.643	470.903
Ravne 3	9	6513026.789	4872410.187	470.896

Continued

Ravne 3	10	6513029.367	4872408.450	470.886
Ravne 3	11	6513036.352	4872410.023	470.755
Ravne 3	12	6513038.193	4872407.731	470.035
Ravne 3	13	6513031.094	4872403.672	470.230
Ravne 3	14	6513020.868	4872398.396	470.661
Ravne 3	15	6513027.252	4872393.828	470.216
Ravne 3	16	6513018.845	4872391.606	470.886
Ravne 3	17	6513018.821	4872385.254	470.728
Ravne 3	18	6513007.619	4872388.329	470.695
Ravne 3	19	6513011.238	4872383.596	470.772
Ravne 3	20	6513007.570	4872379.549	470.739
Ravne 3	21	6513019.951	4872381.175	470.268
Ravne 3	22	6513013.203	4872379.766	470.360
Ravne 3	23	6513018.665	4872382.956	470.284
Ravne 3	24	6513026.955	4872375.399	470.564
Ravne 4	1	6512899.160	4872096.977	471.666
Ravne 4	2	6512913.315	4872102.211	471.399
Ravne 4	3	6512909.878	4872109.218	471.393
Ravne 4	4	6512928.996	4872096.770	470.771
Ravne 4	5	6512928.497	4872099.717	470.762
Ravne 4	6	6512927.451	4872104.452	—
Ravne 4	7	6512937.595	4872100.850	470.656
Ravne 4	8	6512935.154	4872097.580	470.659
Ravne 4	9	6512933.430	4872092.983	471.454
Ravne 4	10	6512943.429	4872101.566	470.519
Ravne 5	1	6513259.014	4872616.664	470.112
Ravne 5	2	6513264.979	4872612.047	470.359
Ravne 5	3	6513263.369	4872607.909	470.222
Ravne 5	4	6513267.618	4872619.950	470.343
Ravne 5	5	6513283.722	4872593.940	470.388
Ravne 5	6	6513284.006	4872589.563	470.488
Ravne 5	7	6513305.116	4872575.666	470.957
Ravne 5	8	6513306.740	4872572.646	471.115
Ravne 5	9	6513308.213	4872569.910	471.238
Ravne 5	10	6513286.665	4872563.475	471.852
Ravne 5	11	6513278.533	4872564.821	471.684
Ravne 5	12	6513275.063	4872566.067	471.693

Continued

Ravne 5	13	6513325.816	4872545.827	471.907
Ravne 5	14	6513338.900	4872533.428	472.299
Ravne 5	15	6513309.110	4872512.750	472.219
Ravne 6	1	6513013.974	4872138.124	471.333
Ravne 6	2	6513026.103	4872125.572	472.625
Ravne 6	3	6513029.628	4872123.355	472.553
Ravne 6	4	6513029.589	4872120.796	472.573
Ravne 6	5	6513023.797	4872114.884	472.615
Ravne 6	6	6513019.317	4872115.036	472.508
Ravne 6	7	6513016.182	4872116.744	472.502
Ravne 6	8	6513014.979	4872115.589	472.477
Ravne 6	9	6513018.805	4872113.015	472.520
Ravne 6	10	6513023.566	4872110.778	472.698
Ravne 6	11	6513025.798	4872110.228	472.697
Ravne 6	12	6513036.100	4872105.032	472.735
Ravne 6	13	6513037.865	4872119.071	472.739
Ravne 6	14	6513034.680	4872114.783	472.692
Ravne 6	15	6513038.767	4872115.087	472.656
Ravne 6	16	6513032.362	4872118.063	472.647
Ravne 6	17	6513027.922	4872116.046	472.647
Ravne 6	18	6513015.435	4872117.569	472.471
Ravne 6	19	6513007.885	4872126.123	472.887
Ravne 6	20	6513016.804	4872119.488	472.490
Ravne 6	21	6513011.985	4872113.558	472.494
Ravne 6	22	6513007.583	4872099.079	472.786
Ravne 6	23	6513005.802	4872117.987	472.630
Ravne 6	24	6513040.766	4872123.703	473.248
Ravne 6	25	6513021.217	4872107.119	472.703
Ravne 6	26	6513029.591	4872105.070	472.659

—No floor level: no surveyed floor point lies within 4 m of the axis point (Ravne 1, points 38 and 58; Ravne 4, point 6; nearest floor points at 5.5, 5.2 and 4.1 m).

S3. Surveyor's Point Lists

S3 consists of the original point lists exported by the surveyor from the terrestrial laser-scanning (TLS) survey of Ravne 1 - 6. There are 18 plain-text files with 25613 points in total. Because of their size, they are not reproduced here. They are sup-

plied as a separate archive, S3_GeoGIS_point_lists.zip, and are listed in Table S3.

Format: one point per line, tab- or space-separated. Columns are point number, Y (easting), X (northing), H (height) and survey code. Some axis files have no height column. In the axis files of Ravne 1 and Ravne 5, H = 0.000 means no height was recorded; these values are not used. File names keep the surveyor's Bosnian labels: TUNEL = tunnel, PLAFON = ceiling, OSOVINA = axis, SUHOZID = dry-stone wall.

The surveyor notes that floor points are mostly on the floor itself but include the gentle slopes where the floor meets the side walls.

Table S3. Inventory of the surveyor's point-list files.

File	System	Content	Survey code	Points
1.1_-_TUNEL_RAVNE_1.txt	Ravne 1	Floor points	500_KOTA	2279
1.1_-_TUNEL_RAVNE_1_-_OSOVINA.txt	Ravne 1	Passage axis points	273_TUNEL_OS	98
1.1_-_TUNEL_RAVNE_1_-_PLAFON.txt	Ravne 1	Ceiling points	500_KOTA_PLAFON	12,059
1.2_-_TUNEL_RAVNE_1_-_SUHOZID.txt	Ravne 1	Dry-stone wall points	SUHOZID_n	30
2.1_-_TUNEL_RAVNE_2.txt	Ravne 2	Floor points	500_KOTA	84
2.1_-_TUNEL_RAVNE_2_-_OSOVINA.txt	Ravne 2	Passage axis points	—	2
3.1_-_TUNEL_RAVNE_3.txt	Ravne 3	Floor points	500_KOTA	1526
3.1_-_TUNEL_RAVNE_3_-_OSOVINA.txt	Ravne 3	Passage axis points	—	24
3.1_-_TUNEL_RAVNE_3_-_PLAFONA.txt	Ravne 3	Ceiling points	500_KOTA_PLAFON	2717
4.1_-_TUNEL_RAVNE_4.txt	Ravne 4	Floor points	500_KOTA	273
4.1_-_TUNEL_RAVNE_4_-_OSOVINA.txt	Ravne 4	Passage axis points	—	10
4.1_-_TUNEL_RAVNE_4_-_PLAFON.txt	Ravne 4	Ceiling points	500_KOTA_PLAFON	484
5.1_-_TUNEL_RAVNE_5.txt	Ravne 5	Floor points	500_KOTA	666
5.1_-_TUNEL_RAVNE_5_-_OSOVINE.txt	Ravne 5	Passage axis points	—	15
5.1_-_TUNEL_RAVNE_5_-_PLAFON.txt	Ravne 5	Ceiling points	500_KOTA_PLAFON	3911
6.1_-_TUNEL_RAVNE_6.txt	Ravne 6	Floor points	500_KOTA	363
6.1_-_TUNEL_RAVNE_6_-_OSOVINA.txt	Ravne 6	Passage axis points	—	26
6.1_-_TUNEL_RAVNE_6_-_PLAFON.txt	Ravne 6	Ceiling points	500_KOTA_PLAFON	1046
Total				25,613

S4. Analysis Script

The Python script below reproduces Tables 2-4 and the Monte Carlo tests of the paper from the S3 point lists. It needs Python 3 with NumPy and SciPy. Run it as:

python S4_analysis.py S3_GeoGIS_point_lists/

The random seed is fixed (20261023), so the output is identical on every run. Blocks headed “if False:” are diagnostic printouts and are switched off by default. The script is also supplied as a separate file, S4_analysis.py.

```
"""S4 - Analysis script for "Was the Ravne Underground Complex Once a Single Network?"
Usage: python S4_analysis.py <folder with GeoGIS .txt point lists>
Requires numpy, scipy. Reproduces Tables 2-4 and the Monte Carlo tests (seed 20261023)."""
import sys
import glob,re,numpy as np
T=(sys.argv[1] if len(sys.argv)>1 else '.').rstrip('/')+'/'
def rd(pat,nh=4):
    f=glob.glob(T+'*'+pat)
    if not f: return np.zeros((0,nh))
    assert len(f)==1,(pat,f)
    out=[]
    for line in open(f[0],errors='replace'):
        nums=[]
        for t in re.split(r'[\t ,;]+',line.strip()):
            try: nums.append(float(t))
            except: pass
        if len(nums)>=3: out.append(nums[:nh])
    return np.array([r+[np.nan]*(nh-len(r)) for r in out])
S={}
for k in range(1,7):
    fl=rd(f'TUNEL_RAVNE_{k}.txt'); ce=rd(f'TUNEL_RAVNE_{k}_-_PLAF*.txt')
    ax=rd(f'TUNEL_RAVNE_{k}_-_OSOVIN*.txt',4)
    S[k]=dict(floor=fl[:,1:4],ceil=ce[:,1:4] if len(ce) else None,axis=ax[:,1:3],axid=ax[:,0].astype(int))
# entrances from paper Table 2 (axis point nearest ULAZ label)
ENT={1:(6513219.88,4872433.48),2:(6513154.86,4872157.67),3:(6513038.19,4872407.73),4:(6512943.43,4872101.57),5
:(6513259.01,4872616.66),6:(6513013.97,4872138.12)}
GEO_LEN={1:1706.5,2:13.9,3:208.9,4:84.4,5:251.3,6:187.7}
GEO_GRAD={1:1.0,2:None,3:0.94,4:1.9,5:1.4,6:2.0}
def classify(k):
    fl=S[k]['floor']; e=np.array(ENT[k]); v=fl[:,:2]-e; d=np.hypot(*v.T)
    ring=(d>=3)&(d<=15)
    u=e-fl[ring,:2].mean(0); u/=np.hypot(*u)
    proj=v@u
    appr=(proj>0.5)&(d<20)
    return appr,d,u
R={}
```

```
for k in S:
    fl=S[k]['floor']; appr,d,u=classify(k)
    inn=~appr
    near=inn&(d<=4)
    ent=np.median(fl[near,2])
    R[k]=dict(ent=ent,lo=fl[inn,2].min(),hi=fl[inn,2].max(),n_in=inn.sum(),n_ap=appr.sum(),
        ap_lo=fl[appr,2].min() if appr.any() else np.nan, ap_hi=fl[appr,2].max() if appr.any() else np.nan, u=u,
n_near=near.sum(), sd_near=fl[near,2].std())
if False:
    for k,r in R.items():
        print(f"R{k}: entrance {r['ent']:.3f} (n={r['n_near']}, sd {r['sd_near']:.3f}) | interior {r['lo']:.3f}-{r['hi']:.3f}
n={r['n_in']} | approach n={r['n_ap']} {r['ap_lo']:.2f}-{r['ap_hi']:.2f} | ent-lo {r['ent']-r['lo']:.3f} hi-ent {r['hi']-r['ent']:.2f}
| facing {np.degrees(np.arctan2(r['u'][0],r['u'][1]))%360:.0f}°")
    es=[r['ent'] for r in R.values()]; print('entrance spread', min(es), max(es), max(es)-min(es))
    print('total interior', sum(r['n_in'] for r in R.values()), 'total', sum(len(S[k]['floor']) for k in S))
from scipy.spatial import cKDTree
from scipy.sparse import coo_matrix
from scipy.sparse.csgraph import dijkstra, connected_components
from scipy.stats import spearmanr
def ENTF(k,r=2.0):
    fl=S[k]['floor']; d=np.hypot(*(fl[:,:2]-np.array(ENT[k])).T); return np.median(fl[d<=r,2])
def geodesic(k,thr):
    fl=S[k]['floor']; ce=S[k]['ceil']
    P=fl[:,:2] if ce is None else np.vstack([fl[:,:2],ce[:,:2]])
    P=np.vstack([P,np.array(ENT[k])[None]])
    t=cKDTree(P); pairs=t.query_pairs(thr,output_type='ndarray')
    w=np.hypot(*(P[pairs[:,0]]-P[pairs[:,1]]).T)
    n=len(P); G=coo_matrix((w,(pairs[:,0],pairs[:,1])),shape=(n,n))
    dist=dijkstra(G,directed=False,indices=n-1)
    return dist[:len(fl)]
G2={}
if False:
  for k in S:
    fl=S[k]['floor']; appr,_,_=classify(k); inn=~appr
    for thr in (2.0,3.0,5.0):
        g=geodesic(k,thr); ok=np.isfinite(g)&inn
        print(f"R{k} thr={thr}: reachable {ok.sum()}/{inn.sum()}   maxdist {g[ok].max():.0f}")
def grad(k,thr=3.0,bw=2.0):
    fl=S[k]['floor']; appr,_,_=classify(k); g=geodesic(k,thr); ok=np.isfinite(g)&~appr
    D,H=g[ok],fl[ok,2]; b=np.floor(D/bw).astype(int)
    ub=np.unique(b); bd=np.array([D[b==i].mean() for i in ub]); bh=np.array([np.median(H[b==i]) for i in ub])
    slope=np.polyfit(bd,bh,1)[0]*100
    rho=spearmanr(D,H).correlation
```

```
    e=ENTF(k); below=(bh<e-0.05).mean()
    # unsigned local slope between consecutive bins
    loc=np.abs(np.diff(bh))/np.diff(bd)*100
    return dict(slope=slope,rho=rho,below=below,nb=len(ub),loc=np.mean(loc),Dmax=D.max(),rise=(H.max()-e))
if False:
  for k in S:
    r=grad(k); print(f"R{k}: signed {r['slope']:+.2f}%  rho {r['rho']:+.2f}  bins below entrance {r['below']*100:.0f}% unsigned-local {r['loc']:.2f}%  GeoGIS {GEO_GRAD[k]}  nbins {r['nb']} Dmax {r['Dmax']:.0f}")
  for bw in (1.0,5.0):
    print(bw,[round(grad(k,bw=bw)['slope'],2) for k in S])
def ends(k,rmin=3,rmax=15,thr=0.75):
    fl=S[k]['floor']; appr,_,_=classify(k); P=fl[~appr,:2]
    out=[]
    for i,(a,pid) in enumerate(zip(S[k]['axis'],S[k]['axid'])):
        v=P-a; d=np.hypot(*v.T); m=(d>=rmin)&(d<=rmax)
        if m.sum()<3: continue
        uv=v[m]/d[m,None]; R=uv.mean(0); L=np.hypot(*R)
        if L>=thr:
            f=-R/L; out.append(dict(sys=k,pt=int(pid),xy=a,face=np.arctan2(f[0],f[1]),L=L))
    return out
E=[e for k in S for e in ends(k)]
XY=np.array([e['xy'] for e in E]); SYS=np.array([e['sys'] for e in E]); FACE=np.array([e['face'] for e in E])
# bearing to nearest axis point of each other system within 300 m
TARG=[]
for e in E:
    tl=[]
    for k in S:
        if k==e['sys']: continue
        A=S[k]['axis']; d=np.hypot(*(A-e['xy']).T); j=d.argmin()
        if d[j]<=300:
            v=A[j]-e['xy']; tl.append((k,np.arctan2(v[0],v[1]),d[j]))
    TARG.append(tl)
def angd(a,b): return np.abs((a-b+np.pi)%(2*np.pi)-np.pi)
def stats(face,tol=35):
    t=np.radians(tol); n=0; offs=[]
    for f,tl in zip(face,TARG):
        if any(angd(f,b)<=t for _,b,_ in tl): n+=1
        if tl:
            near=min(tl,key=lambda z:z[2]); offs.append(angd(f,near[1]))
    return n,np.degrees(np.mean(offs))
# mutual pairs
PD=np.hypot(*(XY[:,None]-XY[None]).transpose(2,0,1))
BR=np.arctan2(XY[None,:,0]-XY[:,None,0],XY[None,:,1]-XY[:,None,1])  # bearing i->j
```

```
DIFF=SYS[:,None]!=SYS[None]
def mutual(face,dmax=100,tol=35):
    t=np.radians(tol)
    a=angd(face[:,None],BR)<=t
    m=a&a.T&DIFF&(PD<dmax)
    return int(np.triu(m,1).sum())
if False:
    for k in S: print(k, len([e for e in E if e['sys']==k]), [e['pt'] for e in E if e['sys']==k])
    print('ends',len(E))
    for tol in (35,10,15,20): print(tol, stats(FACE,tol))
    print('excl R1', stats(FACE[SYS!=1],35) if False else '')
    print('mutual', mutual(FACE))
def stats2(face,tol=35,mask=None):
    t=np.radians(tol); n=0; offs=[]
    for i,(f,tl) in enumerate(zip(face,TARG)):
        if mask is not None and not mask[i]: continue
        if not tl: continue
        a=[angd(f,b) for _,b,_ in tl]
        if min(a)<=t: n+=1
        offs.append(min(a))
    return n,np.degrees(np.mean(offs))
def mutual_list(face,dmax=100,tol=35):
    t=np.radians(tol); a=angd(face[:,None],BR)<=t
    m=np.triu(a&a.T&DIFF&(PD<dmax),1); return [(E[i],E[j],PD[i,j]) for i,j in zip(*np.nonzero(m))]
def axis_xy(k,pt): return S[k]['axis'][list(S[k]['axid']).index(pt)]
EPT={1:1,2:1,3:12,4:10,5:1,6:1}
def floor_at(k,xy,r=4):
    fl=S[k]['floor']; appr,_,_=classify(k); d=np.hypot(*(fl[:,:2]-xy).T); m=(d<=r)&~appr
    return np.median(fl[m,2])
def endface(k,pt):
    for e in E:
        if e['sys']==k and e['pt']==pt: return e['face']
    return None
LINKS=[('L1',(1,35),(5,15)),('L2',(5,14),(1,37)),('L3',(4,10),(6,23)),('L4',(6,24),(1,94)),('L5',(3,12),(1,1)),('L6',(1,97),(6,2
4)),('L7',(3,24),(2,1))]
def link(a,b):
    A=axis_xy(*a); Bx=axis_xy(*b)
    fa=ENTF(a[0]) if a[1]==EPT[a[0]] else floor_at(a[0],A)
    fb=ENTF(b[0]) if b[1]==EPT[b[0]] else floor_at(b[0],Bx)
    D=np.hypot(*(Bx-A)); dH=abs(fa-fb)
    al=[]
    for (k,p),src,dst in ((a,A,Bx),(b,Bx,A)):
        f=endface(k,p); al.append(None if f is None else np.degrees(angd(f,np.arctan2(*(dst-src)))))
```

```
    return dict(A=A,B=Bx,fa=fa,fb=fb,D=D,dH=dH,S=dH/D*100,al=al)
if False:
    for n,a,b in LINKS:
        r=link(a,b); print(n,a,b,f'D {r['D']:.1f} fa {r['fa']:.3f} fb {r['fb']:.3f} dH {r['dH']:.2f} S {r['S']:.2f} align {r['al']}")
rng=np.random.default_rng(20261023)
NE=len(E); M=max(len(t) for t in TARG)
B=np.full((NE,M),np.nan)
for i,t in enumerate(TARG):
    for j,(_,b,_) in enumerate(t): B[i,j]=b
A_mut=np.triu(DIFF&(PD<100),1); I,J=np.nonzero(A_mut)
def batch(F):
    # F: (n,NE) faces
    off=angd(F[:,:,None],B[None]); off=np.where(np.isnan(B)[None],np.inf,off); mn=off.min(2)
    res={f'c{t}':(mn<=np.radians(t)).sum(1) for t in (10,15,20,35)}
    res['moff']=np.degrees(mn.mean(1)); res['cR']=(mn[:,SYS!=1]<=np.radians(35)).sum(1)
    ai=angd(F[:,I],BR[I,J][None])<=np.radians(35); aj=angd(F[:,J],BR[J,I][None])<=np.radians(35)
    res['mut']=(ai&aj).sum(1); return res
obs=batch(FACE[None]); obs={k:v[0] for k,v in obs.items()}
def gen(model,n):
    if model=='uniform': return rng.uniform(-np.pi,np.pi,(n,NE))
    F=np.empty((n,NE))
    for k in S:
        idx=np.where(SYS==k)[0]
        if model=='rotation': F[:,idx]=FACE[idx][None]+rng.uniform(-np.pi,np.pi,(n,1))
        else: F[:,idx]=FACE[idx][rng.permuted(np.tile(np.arange(len(idx)),(n,1)),axis=1)]
    return F
OUT={}
for model in ('uniform','rotation','permutation'):
    acc={}
    for _ in range(10):
        r=batch(gen(model,10000))
        for k,v in r.items(): acc.setdefault(k,[]).append(v)
    acc={k:np.concatenate(v) for k,v in acc.items()}
    OUT[model]=acc
    print(f"== {model}")
    for k in ('c35','c10','c15','c20','cR','mut'):
        print(f"  {k}: obs {obs[k]}  null {acc[k].mean():.1f} ± {acc[k].std():.1f}  p(>=obs) {(acc[k]>=obs[k]).mean():.3f}" + (f"  p(>=1) {(acc[k]>=1).mean():.3f}" if k=='mut' else ''))
    print(f"  moff: obs {obs['moff']:.1f}  null {acc['moff'].mean():.1f}  p(<=obs) {(acc['moff']<=obs['moff']).mean():.3f}")
```